Sensors & Actuators: B. Chemical 448 (2026) 138936

Contents lists available at ScienceDirect

Sensors and Actuators: B. Chemical

journal homepage: www.elsevier.com/locate/snb

Methylamine gas sensing by optical array

Alessia Cavallaro [a], Rossella Santonocito [a], Andrea Pappalardo [a,b], Nunzio Tuccitto [a,*], Giuseppe Trusso Sfrazzetto [a,b,**]

[a] Department of Chemical Sciences, University of Catania, Viale A. Doria 6, Catania 95125, Italy
[b] INSTM Udr of Catania, Viale Andrea Doria 6, Catania 95125, Italy

ARTICLE INFO

Keywords:
Array
Diagnostics
Methylamine
Fluorescence
Optical fiber

ABSTRACT

Methylamine (MA) represents a threat to human health due to its toxic effects and potential improper use in illicit activities, requiring a sensitive and selective method for its detection. In this work, MA sensing in gas phase has been performed using an optical array, consisting of several organic fluorescent probes, combined with an optical fiber as detector. Precise control of gas concentration has been provided using a gas permeator, which provides a highly stable and reproducible stream of MA. The combination of this system and our optical array leads, compared with other optical sensors, to the lowest linear detection range of 100–1000 ppb, and also, an excellent performance in normal atmospheric conditions. Moreover, the array method exhibits an excellent selectivity in the presence of humidity and other structurally similar molecules.

1. Introduction

Methylamine (MA) is the simplest primary amine, and it derives from ammonia, bearing a methyl group in place of a hydrogen. MA appears like a colorless, flammable water-soluble gas, with a characteristic ammonia pungent odor when it reaches concentrations above 100 ppm [1]. MA can be released from both natural and anthropogenic sources, including industries [2], tobacco smoke [3], fish processing [4], and livestock [5], where it is present as a result of biological degradation of nitrogen-containing compounds. Also, it is employed as a precursor in the illicit production of methamphetamine [6]. Exposure to gaseous MA usually occurs through inhalation in workplaces where it is produced, handled, or stored, particularly under inadequate ventilation or during accidental releases. This will entail eye, nose and throat irritation at concentrations around 20–100 ppm [7], while at higher concentrations its inhalation may lead to breathing difficulty, pulmonary edema and cardiac palpitations. Repeated exposure may result in liver damage and chronic bronchitis [8]. Moreover, MA can be adsorbed through various routes, including the respiratory and gastrointestinal tracts as well as the skin. Once in the body, it can undergo metabolic conversion into dimethylamine or be oxidized to formic acid, both of which are associated with significant toxicity [9]. To protect workers and public health, national and international agencies established exposure limits for MA at gas phase: World Health Organization (WHO), European Food Safety Authority (EFSA) and U.S. Food and Drug Administration (FDA) agree that the recommended exposure limit (REL-TWA) is 10 ppm [10]. In this context, the development of a sensitive and selective method for the detection of trace gaseous MA becomes crucial to provide accurate monitoring and safeguard human health.

Even though various techniques are used for MA sensing, such as liquid and gas chromatography [11], quartz crystal microbalance [12] and electrochemical methods [13,14], they are impractical for point-of-need monitoring, because their application represents a huge investment in terms of instruments, technology and skilled operators. Furthermore, they require sample preparation, and the time needed for a single analysis may be relevant and not useful to detect the presence of gaseous MA in real time. To overcome these issues, optical sensors have attracted great attention due the simple identification of variations with naked eye [15]. Among them, fluorescent sensors have been reported for MA sensing, because they represent a good approach for environmental monitoring, enabling to meet the demand for easy, rapid, cost-effective, sensitive and selective detection [16–19]. Indeed, for sensing applications, selectivity plays a crucial role, especially when complex environmental matrices are analysed. Selectivity can be gained using an optical array sensor, a sensing platform that contains a high number of probes, each one capable to interact with analytes via non-covalent interactions [20,21], in a portable ready-to-use device. Unlike traditional sensors that are specifically tailored to detect a single target, array-based

* Corresponding author.
** Corresponding author at: Department of Chemical Sciences, University of Catania, Viale A. Doria 6, Catania 95125, Italy.
E-mail addresses: nunzio.tuccitto@unict.it (N. Tuccitto), giuseppe.trusso@unict.it (G. Trusso Sfrazzetto).

https://doi.org/10.1016/j.snb.2025.138936
Received 4 September 2025; Received in revised form 1 October 2025; Accepted 8 October 2025
Available online 8 October 2025

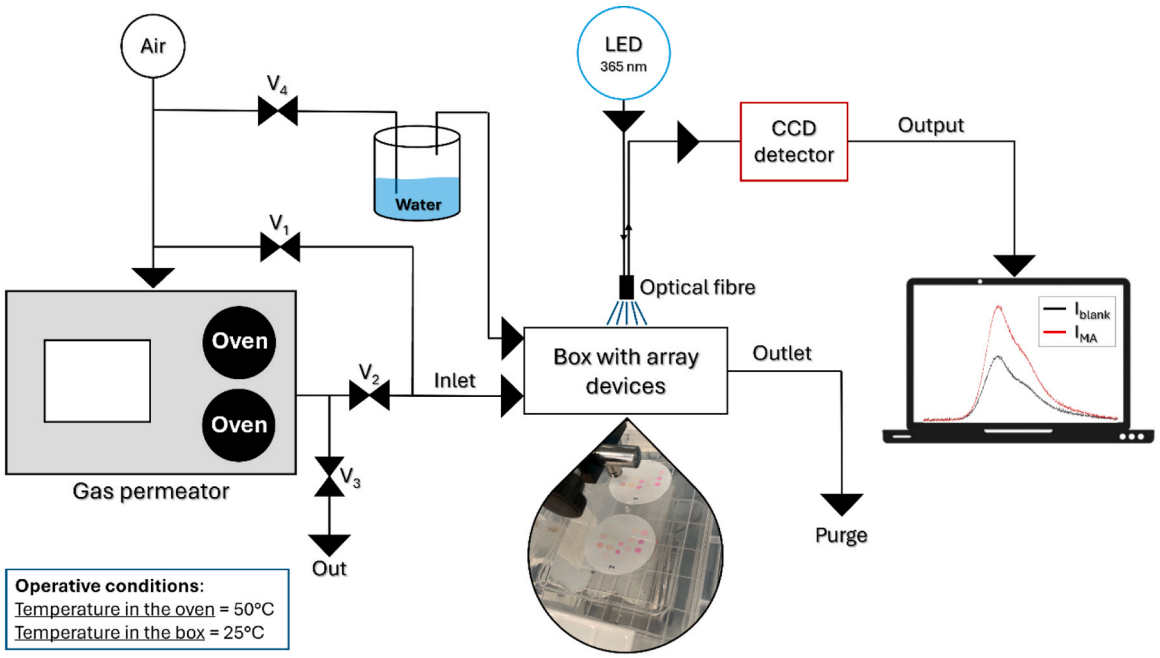

Fig. 1. Schematic representation of the experimental setup built for MA detection.

systems allow for differential interactions with a wide range of compounds, even when applied to challenging matrices, typical of environmental systems [22]. The collective optical response of all probes needs to be processed through multivariate statistical analysis to extract meaningful information, and results in a unique fingerprint for each analyte, thus enhancing selectivity towards the chosen analyte [23–25].

Herein, we present an optical array sensor made up of organic fluorescent probes, able to identify and quantify gaseous MA in real environmental matrices, reaching an experimental limit of detection as low as 100 ppb (the lowest MA concentration used in this work), well below the limit threshold imposed by health authorities. Moreover, the prediction of an unknown sample was evaluated using machine learning algorithms. To the best of our knowledge, the reported system represents the first case in which a fluorescent array sensor is employed to detect MA. In addition, our device detects MA in gas phase with the lowest concentration linear range (100 – 1000 ppb).

2. Experimental section

2.1. Preparation of the array

Several circular supports in polyamide (5 cm diameter, 0.2 μm pore size) underwent UV/O_3 treatment, to purify and activate their surface before the deposition of the fluorescent probes. The probes were drop casted in different positions of the support, 1.5 μL of 1 mM solution in $CHCl_3$ per each, except for phenanthrene (1.5 μL of a 0.5 M solution in $CHCl_3$), and the solvent was allowed to evaporate at room temperature The arrays were laid one day for stabilization before any use.

2.2. Experimental setup

The experimental setup (Fig. 1) built for the measurements consists of a transparent box, where three identical arrays were placed, by attaching them to the lid's inner surface. Different gaseous MA concentrations are generated using a gas calibrator (PermaCal, from LNI Swissgas SA, Switzerland), that operates by diluting a 100 % pure CH_3NH_2 gas source compressed in permeation tubes with a carrier gas (nitrogen for the array calibration and air for the other analyses). Likewise, for the interferents, 100 % pure gas sources of hydrogen

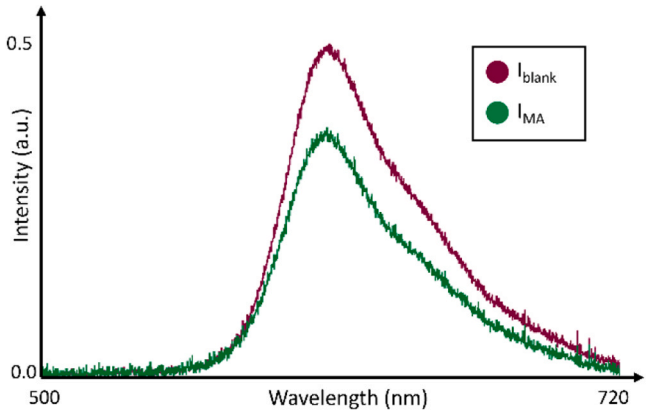

Fig. 2. Overlap of emission spectra of one representative probe: blank spectrum is reported in red, and the probe's spectrum after exposure to MA is reported in green.

sulfide, ethyl mercaptan and ammonia were employed and diluted with carrier gas as previously described for MA. When the permeation tube is maintained at a constant temperature of 50 °C inside the oven, the weight of both the permeating and evaporating diffusion gases remains steady, making the instrument a fundamental tool to have an accurate control over the final analyte concentration in the gaseous stream [26], in a range between 100 and 1000 ppb.

The box with the array devices is equipped with a hygrometer, that provides the values of relative humidity (RH %) and temperature during all the experiments. Each measurement, performed at 25 °C inside the box, is carried out in two steps that result in two different configurations of the system: stream stabilization (blank) and injection of the analyte (inject). Stream stabilization and analyte injection procedures were carefully optimized to ensure reproducibility and accurate sensitivity/selectivity measurements. During the blank phase, a stable carrier gas flow was passed through the optical array while monitoring the baseline fluorescence response until full stabilization. Once the baseline was constant, the system was switched to the injection phase, in which a known concentration of methylamine gas was introduced using a

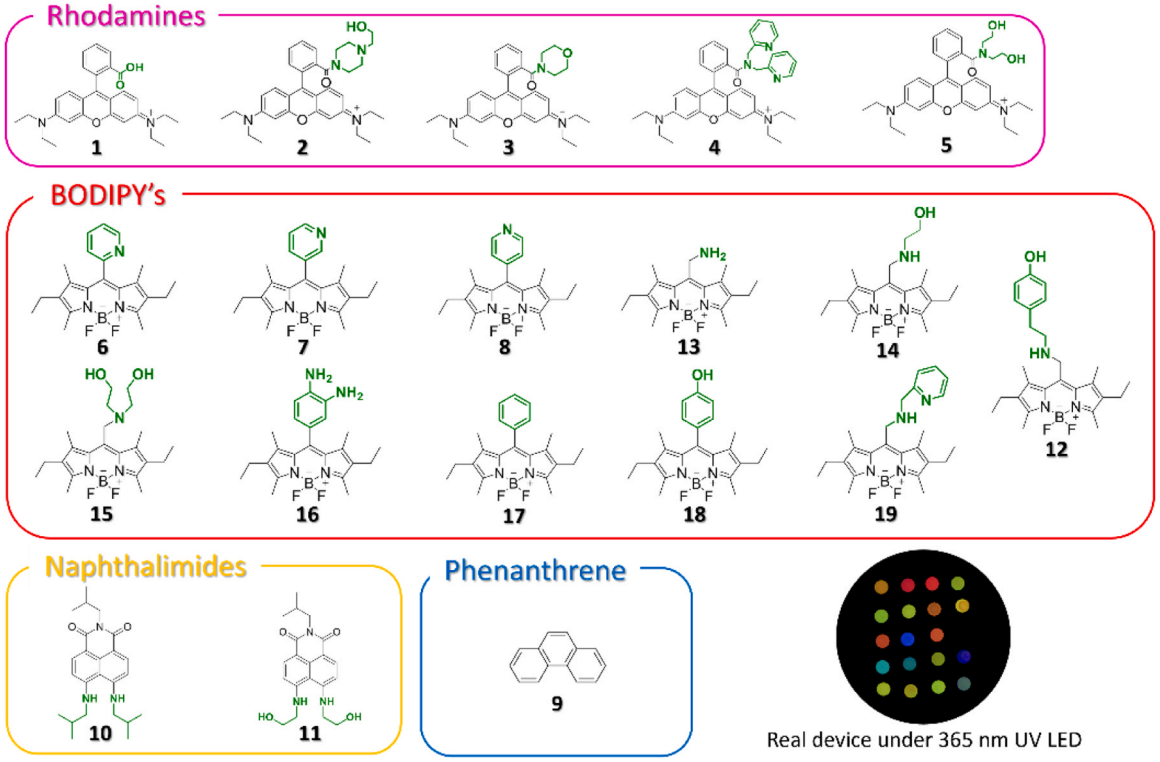

Fig. 3. Layout of molecular probes in the optical array, divided into fluorophores families: the fluorescent cores are reported in black, and the recognition sites are highlighted in green. The real device under 365 nm UV LED irradiation is shown in the bottom right of the figure.

calibrated gas permeator device. This setup ensured a highly stable and reproducible analyte concentration reaching the sensing chamber. In particular, during the stabilization phase, only valves V_1 and V_3 (Fig. 2, on the left) are open; in this configuration, air flows into the box, while MA-enriched stream from the permeator is directed to waste. Once the target flow conditions are stabilized (it takes one night), the gas flow is diverted into the chamber by switching the valves configuration: valves V_1 and V_3 are closed, and valve V_2 is open, letting the gaseous analyte at the desired concentration to reach the array sensors inside the chamber. Valve V_4 is closed during calibration experiments. It is opened only when measurements at high humidity are performed. In particular, in order to generate such levels of humidity, a parallel air stream must be directed to a bubbler filled with water, which produces a maximum relative humidity of 70 % inside the box, as measured with a hygrometer. The characterization of Hyperspectral Ultraviolet-Induced Visible Fluorescence Mapping (HUVFM) was conducted using a custom-built instrument (Fig. 1, on top). The optical fiber employed, acquired from Thorlabs, features a pure silica core with a fluorine-doped silica cladding with high hydroxyl ion concentrations, and a total diameter of 220 μm, including core and cladding. The analysis probe consists of a bundle of 19 Y-shaped fibers (BF19Y2HS02 sourced from Thorlabs), provided with a beam collimator (F220SMA-532 sourced from ThorLabs) separated by the box lid from the analysis point. Among the 19 fibers, 10 are Y-ends connected to the source, which is a 365 nm LED sourced from Thorlabs. The remaining 9 fibers are linked to an optical block housing bandpass filter sourced from, designed to block backscattered light from the source. Subsequently, the CCD detector (CCS100/M sourced from Thorlabs) is connected to a bundle of optical fibers arranged linearly (BFL200HS02 sourced from Thorlabs), maximizing the light collected by the sampling led.

2.3. Data collection and elaboration

First, fluorescence intensity data were collected for the blank, that is the emission of probes before exposure to any analyte (I_{blank}). Second, we let MA enter the chamber with the array devices and collected the fluorescence intensity of the probes after exposure to the gaseous analyte (I_{MA}). A representative comparison between the two spectra is shown in Fig. 2.

In order to provide the dataset to the software that performs multivariate analysis, fluorescence intensity data were processed according to the following formula, where *N. I.* indicates the *Normalized Intensity*:

$$N.I. = \frac{I_{MA}}{I_{blank}}$$

This simple ratio enables the normalization with the contribution due to the blank signal, providing the intensity variation associated with each probe after exposure to the analyte.

3. Results and discussion

The designed optical array sensor is made up of 19 fluorescent organic molecules, each featuring two functional parts: a fluorophore, which enables detection by fluorescence, and a recognition site, which establishes non-covalent interactions with the analyte. The selected fluorophores are BODIPY's, rhodamines, naphthalimides and phenanthrene derivatives. These fluorescent cores were chosen due to their wide absorption ranges, distinct emission ranges within the visible spectrum and the possibility to be excited by UV light at 365 nm. In particular, this excitation wavelength interacts with the conjugated aromatic portion of the chromophore, leading to π-π* transition. In detail, rhodamines were selected because they absorb in the range between 500 and 600 nm and emit between 550 and 650 nm; they were functionalized with recognition sites capable of forming hydrogen bonds with MA. BODIPY derivatives were chosen due to their strong absorption around 500 nm and emission that covers the 500–700 nm range, depending on the functionalization. They were modified with groups able to form hydrogen bonds as well as CH-π interactions with the analyte.

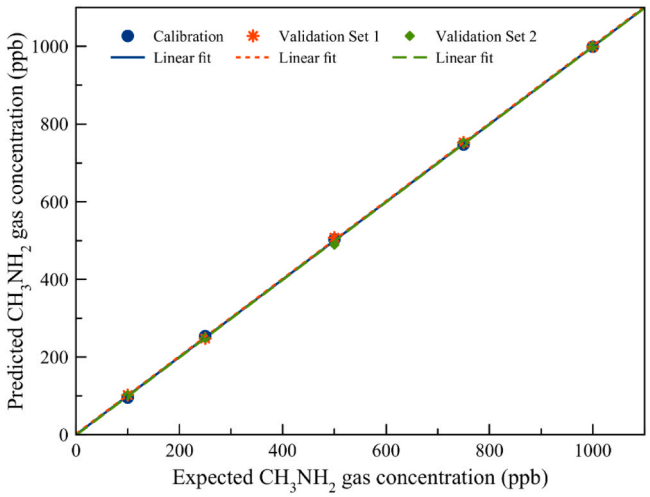

Fig. 4. Expected CH_3NH_2 gas concentration *vs* Predicted CH_3NH_2 gas concentration expressed in ppb and calculated using PLS model with 5 PCs (blue dots). Validation datasets are reported in orange stars and green diamonds.

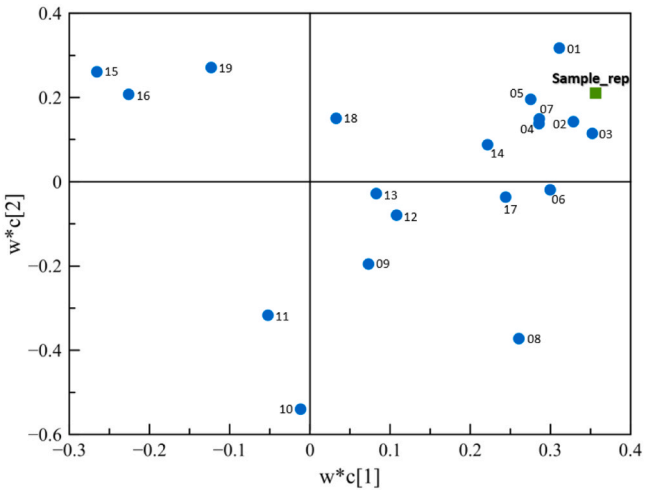

Fig. 5. Loadings plot form PLS model, w*c [1] vs w*c [2]. The light blue circles are the probes, while the green square is the target variable, representing MA concentration.

Naphthalimides absorb in the 340–385 nm region and emit at 450–460 nm. They were functionalized with groups capable of hydrogen bonding and CH-π interactions with MA. Finally, phenanthrene was selected because it absorbs mainly in the 300–340 nm region and emits in the 340–380 nm range; it can interact with methylamine through CH-π interactions [21].

The recognition sites were picked basing on their ability to engage in non-covalent interactions, such as hydrogen bonding, ion-dipole and dipole-dipole interactions. The probes, with their molecular structure, are reported in Fig. 3, divided into fluorophores families, with the fluorescent core reported in black, while the recognition sites are highlighted in green.

Syntheses and characterization of the probes are extensively discussed in the Supplementary Material. In particular, methylamine contains a hydrogen bond acceptor group (nitrogen atom) and two hydrogens able to act as donor groups. The recognition sites introduced in the chromophore of the array contain several complementary groups able to interact with MA by one or more hydrogen bonds.

The box where the array devices are placed (Fig. 1) is not fully sealed. In fact, it includes an outlet hole which ensures that gas does not accumulate inside. This design allows to work in a condition of constant flow rate, preventing the buildup of high analyte concentrations and enabling to have a controlled exposure, thus enhancing reproducibility. Moreover, the transparency of the chamber makes possible external fluorescence measurements of the probes, without the need to open it, with the risk of losing its internal environment.

The optical fiber, used for the optical analyses, has the dual purpose of delivering the excitation light from the LED to the array's probes and of simultaneously collecting their emission, sending it to a CCD, which converts the optical signal into an electric one. This allows to obtain the full spectrum of the probes, then visualized in a computer. In particular, we collected for each probe a spectrum during the stabilization phase, when the arrays are exposed only to gas carrier, whose emission maximum is labeled as I_{blank}, and a spectrum when the arrays have been exposed to gaseous MA for 1 h, to capture the sensor's response to the analyte, with the emission maximum indicated as I_{MA}. For example, Figure S1 (see Supplementary Material) shows a strong quenching of the emission the optical spectra of probe 2, the most correlated to MA quantification, obtained before and after the presence of MA (500 ppb). The response of each probe has been evaluated, showing that at low MA concentration values, rhodamines present the major change of the emission (see Supplementary Material, Figure S2).

Array calibration with MA concentration values of 100 ppb, 250 ppb, 500 ppb, 750 ppb and 1000 ppb was firstly performed. The different MA concentration values are obtained by proper setup of the permeator, which is able to finely tune the desired concentration of the gaseous analyte. Normalized intensity values for each concentration, obtained as reported in the Supplementary Material, were elaborated through multivariate statistical analysis. In particular, Partial Least Squares (PLS) model was applied using 5 principal components (PCs) to obtain a response of the array to gaseous MA in the above-mentioned range, showing an excellent linearity, with $R^2 = 0.9998$ (Fig. 4, blue spots and line). Two more test sets were imported as validation datasets, to understand if these independent measurements are in accord to those used to train the PLS algorithm. The found data are perfectly stackable to the calibration, showing similar values in the investigated range, with R^2 of 0.9998 and 0.9996, respectively (Fig. 4, orange stars and line, green diamonds and line), thus demonstrating the high reproducibility of the method. The values obtained as outcomes of multivariate analysis are reported in Table S1 (see Supplementary Material).

We applied loadings plot from PLS, in order to identify which variables best quantify MA (Fig. 5). In particular, each variable represents one of the fluorescent probes of the array, and its position in the plot reflects its contribution to the quantification of the gaseous analyte. Variables which are highly correlated appear closer in the graph because they have similar weights. In fact, those located closer to the target variable "Sample_rep" are the most strongly statistically correlated with MA concentration. From the plot, we observed that probe 2 (a rhodamine with an ethyl piperazine as recognition site) is the variable that best quantifies MA. Also note that probes 1, 3, 4 and 5 are located close to the "Sample_rep" variable, and they are all rhodamines. This may suggest that the interaction between MA and the recognition sites of rhodamines drastically changes the emission of the fluorescent core, supporting the response results showed in Figure S2 (see Supplementary Material). In particular, all these rhodamine probes contain heteroatoms (i.e., oxygens and nitrogens) in the recognition site able to form hydrogen bonds with the hydrogen contained in MA. The formation of these hydrogen bonds leads to a PET mechanism due to the MA coordination by the lone pairs of these heteroatoms [27].

Comparison between pre- and post- exposure emission spectra of probe 2 at a representative concentration of 500 ppb is reported in the Supplementary Material (Figure S1).

Then, we evaluated the cross sensitivity, in particular the effect of the matrix, including the relative humidity (RH%), on the array sensor's performances and if it could affect MA identification and quantification. In detail, we tested the ability of our array to detect traces of MA in the

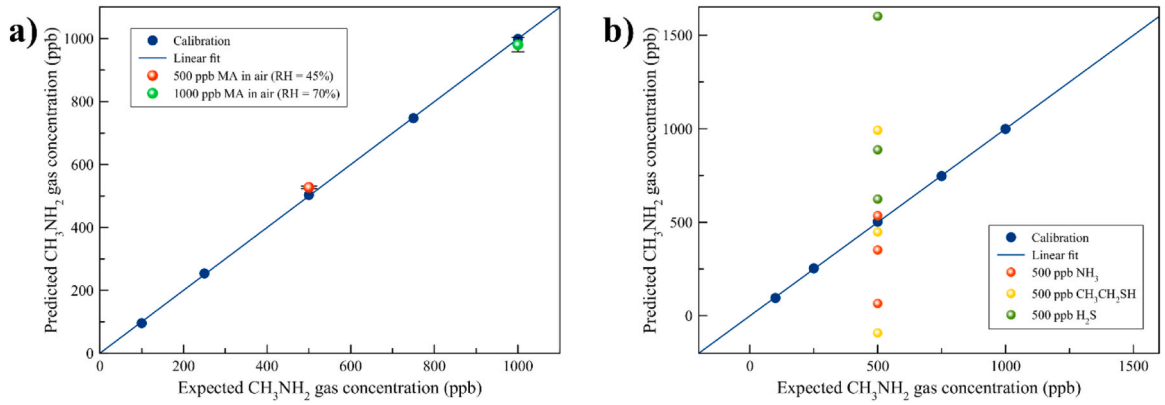

Fig. 6. Calibration points and relative linear fit of MA concentration within the range 100–1000 ppb in nitrogen, represented as blue dots and line, respectively. a) Red dot represents the array's response to MA concentration of 500 ppb in air (RH = 45 %), green dot represents the array's response to MA concentration of 1000 ppb in air (RH = 70 %), each one as an average of three independent replicates, with respective error bars. b) selectivity test: red, yellow and green dots represent 500 ppb of NH_3, CH_3CH_2SH and H_2S in ambient air, respectively.

Table 1
Values obtained from PLS model for MA detection experiments in air, with different RH%.

Expected CH_3NH_2 gas conc. (ppb)	RH = 45 %	Expected CH_3NH_2 gas conc. (ppb)	RH = 70 %
500	518.5	**1000**	990.1
500	534.5	**1000**	928.1
500	528.8	**1000**	1023.7

real atmosphere, containing all real common interferents. Two sets of measurement were carried out with MA concentration of (i) 500 ppb and RH 45 %; (ii) 1000 ppb with RH 70 %, using actual ambient air as gas carrier. The data extracted from the array under these new conditions were used as secondary datasets and compared to the PLS calibration model (Fig. 4). Fig. 6a shows the PLS model, where the dots represent the replicates: we can observe that the concentrations predicted by the PLS model are very close to the real concentrations used (Table 1). Basing on these results, we can affirm that the sensor array performance in the MA detection and quantification is not significantly affected by the matrix and the humidity. We note that these experiments have been performed in different months (32 weeks apart), demonstrating the long-term stability of the sensor.

Finally, selectivity experiments were carried out by exposing the sensor arrays to three different gaseous pollutants, namely ammonia (NH_3), ethyl mercaptan (CH_3CH_2SH) and hydrogen sulfide (H_2S), each tested at a concentration of 500 ppb, and making three replicates per gas. These interferents have been selected as gaseous hydrogen bond donors (ethyl mercaptan and hydrogen sulfide) and simplest nitrogen-based gas. As before, data collected from these measurements were used as secondary dataset and compared to the calibration model trained with MA. As shown in Fig. 6b, these three interferents gave us a different array response respect to MA, highlighting the discriminating ability of our array. In particular, random output values were obtained for all three gases (see Supplementary Material, Table S2), confirming the specificity of this method.

4. Conclusions

In conclusion, the development of an innovative optical array sensor for gaseous MA detection and quantification is here reported. The sensor is able to quantify MA in an experimental range between 100 and 1000 ppb, reaching the lowest experimental LOD compared to previous works. Also, it shows selectivity with respect to other common volatile pollutants contained in air, and it is not affected by the presence of similar gaseous molecules and humidity at different percentages. We are working on the analyses *in-situ* and recovery test. However, due to the low cost of each array device (ca. 5€), probably the "disposable mode" is more convenient respect to the restore of the device. This work paves the way to the development of a fast, easy and selective method to detect and quantify methylamine in real atmospheric condition. It is important to highlight that a real-world application of this sensor will require a proper calibration step performed under atmospheric conditions that closely mimic the sampling environment, but in the absence of methylamine. This calibration step is crucial to eliminate matrix effects arising from the presence of non-target atmospheric components (such as CO_2, N_2, and others) as well as from temperature fluctuations, thereby ensuring reliable and reproducible quantification of methylamine levels.

CRediT authorship contribution statement

Nunzio Tuccitto: Supervision, Data curation, Conceptualization. **Giuseppe Trusso Sfrazzetto:** Writing – original draft, Supervision, Conceptualization. **Rossella Santonocito:** Investigation, Data curation. **Andrea Pappalardo:** Formal analysis. **Alessia Cavallaro:** Investigation, Formal analysis, Data curation.

Declaration of Competing Interest

The authors declare that they have no known competing financial interests or personal relationships that could have appeared to influence the work reported in this paper.

Acknowledgments

This work has been partially funded by European Union (NextGeneration EU), through the MUR-PNRR project SAMOTHRACE (ECS00000022).

Appendix A. Supporting information

Supplementary data associated with this article can be found in the online version at doi:10.1016/j.snb.2025.138936.

Data availability

Data will be made available on request.

References

[1] Compressed Gas Association Inc., Handbook of compressed gases, Ch. 39 (Springer, Boston, 4th Edition, 1999).

[2] Y. Miron, Thermal decomposition of monomethylamine nitrate, J. Hazard. Mater. 3 (1980) 301–321, https://doi.org/10.1016/0304-3894(80)80003-3.

[3] Y. Zhang, J. Mao, P.H. Yu, S. Xiao, A micro trapping system coupled with a high-performance liquid chromatography procedure for methylamine determination in both tissue and cigarette smoke, Anal. Chim. Acta 752 (2012) 106–111, https://doi.org/10.1016/j.aca.2012.09.027.

[4] P. Ma, Z. Zhang, W. Xu, Z. Teng, Y. Luo, C. Gong, Q. Wang, Integrated portable Shrimp-Freshness prediction platform based on ice-templated metal–organic framework colorimetric combinatorics and deep convolutional neural networks, ACS Sustain. Chem. Eng. 9 (2021) 16926–16936, https://doi.org/10.1021/acssuschemeng.1c04704.

[5] G.L. Hutchinson, A.R. Mosier, C.E. Andre, Ammonia and amine emissions from a large cattle feedlot, J. Environ. Qual. 11 (1982) 288–293, https://doi.org/10.2134/jeq1982.00472425001100020028x.

[6] K. Murugappan, C. Kang, D.S. Silvester, Electrochemical oxidation and sensing of methylamine gas in room temperature ionic liquids, J. Phys. Chem. C. 118 (2014) 19232–19237, https://doi.org/10.1021/jp5061045.

[7] G.D. Clayton, F.E. Clayton, Patty's Industrial Hygiene and Toxicology, third ed., Wiley, New York, 1981.

[8] W. Deichmann, H. Gerarde, Toxicology of Drugs and Chemicals, Academic Press, New York, 1969 (12).

[9] J.L. Smith, J.S. Wishnok, W.M. Deen, Metabolism and excretion of methylamines in rats, Toxicol. Appl. Pharmacol. 125 (1994) 296–308, https://doi.org/10.1006/taap.1994.1076.

[10] Occupational Safety and Health Administration (OSHA), Chemical Data – methylamine (Substance No. 558). Available at: https://www.osha.gov/chemicaldata/558 (last updated 2021).

[11] S.T. Chan, M.W.Y. Yao, Y.C. Wong, T. Wong, C.S. Mok, D.W.M. Sin, Evaluation of chemical indicators for monitoring freshness of food and determination of volatile amines in fish by headspace solid-phase microextraction and gas chromatography-mass spectrometry, Eur. Food Res. Technol. 224 (2006) 67–74, https://doi.org/10.1007/s00217-006-0290-4.

[12] K. Zhang, R. Hu, G. Fan, G. Li, Graphene oxide/chitosan nanocomposite coated quartz crystal microbalance sensor for detection of amine vapors, Sens. Actuators B Chem. 243 (2017) 721–730, https://doi.org/10.1016/j.snb.2016.12.063.

[13] K. Murugappan, D.S. Silvester, Sensors for highly toxic gases: methylamine and hydrogen chloride detection at low concentrations in an ionic liquid on pt screen printed electrodes, Sensors 15 (2015) 26866–26876, https://doi.org/10.3390/s151026866.

[14] M. Imran, E.-B. Kim, T.-G. Kim, S. Ameen, M.S. Akhtar, D.-H. Kwak, Fabrication of tungsten oxide nanowalls through HFCVD for improved electrochemical detection of methylamine, Micromachines 15 (2024) 441, https://doi.org/10.3390/mi15040441.

[15] Y. Huang, S. Wang, Y. Zhu, F. Li, J. Jin, J. Dong, F. Lin, Y. Wang, X. Chen, Dual-Mode of fluorescence Turn-On and Wavelength-Shift for methylamine gas sensing based on Space-Confined growth of methylammonium lead tribromide perovskite nanocrystals, Anal. Chem. 92 (2020) 5661–5665, https://doi.org/10.1021/acs.analchem.0c00698.

[16] W. Yin, H. Wang, B. Deng, F. Ma, J. Zhang, M. Zhou, H. Wang, Y. Lu, A pyrylium salt-based fluorescent probe for the highly sensitive detection of methylamine vapour, Analyst 147 (2022) 3451–3455, https://doi.org/10.1039/D2AN00911K.

[17] Y.-Y. Wang, L. Song, S.-Y. Tang, Z.-Q. Dai, J.-Y. Guo, H.-Y. Shen, W.-X. Chai, Highly sensitive and selective gas sensing of methylamine and aniline with a new ternary europium complex material, Mater. Today Commun. 32 (2022) 104054, https://doi.org/10.1016/j.mtcomm.2022.104054.

[18] C. Zhang, Z. Wang, T. Chen, M. Tang, J. Zhang, J. Jian, Y. Wang, K. Zhou, X. Zhang, Methylamine gas sensor based on fluorescent perovskite nanocrystal nanofibers incorporating aggregation-Induced emission materials, ACS Appl. Nano Mater. 7 (2024) 17329–17338, https://doi.org/10.1021/acsanm.4c02342.

[19] Y. Li, X. Tan, S. Wu, W. Hong, J. Luo, S. Zhao, L. Sun, J. Lin, Q. Chen, M. Zhang, Dual-emission ratiometric fluorescence sensor based on in situ formation of $MAPbBr_3$ perovskite nanocrystals in europium metal-organic frameworks for detection of methylamine gas, Sens. Actuators B Chem. 426 (2025) 137092, https://doi.org/10.1016/j.snb.2024.137092.

[20] Z. Li, K.S. Suslick, The optoelectronic nose, Acc. Chem. Res. 54 (2020) 950–960, https://doi.org/10.1021/acs.accounts.0c00671.

[21] R. Santonocito, R. Parlascino, A. Cavallaro, R. Puglisi, A. Pappalardo, F. Aloi, A. Licciardello, N. Tuccitto, S.O. Cacciola, G. Trusso Sfrazzetto, Detection of plant pathogenic fungi by a fluorescent sensor array, Sens. Actuators B. 393 (2023) 134305, https://doi.org/10.1016/j.snb.2023.134305.

[22] R. Santonocito, N. Tuccitto, V. Cantaro, A.B. Carbonaro, A. Pappalardo, V. Greco, V. Buccilli, P. Maida, D. Zavattaro, G. Sfuncia, G. Nicotra, G. Maccarrone, A. Gulino, A. Giuffrida, G. Trusso Sfrazzetto, Smartphone-assisted sensing of trinitrotoluene by optical array, ACS Omega 7 (2022) 37122–37132, https://doi.org/10.1021/acsomega.2c02958.

[23] A. Cavallaro, R. Santonocito, R. Puglisi, A. Pappalardo, F. La Spada, R. Parlascino, M. Riolo, S.O. Cacciola, N. Tuccitto, G. Trusso Sfrazzetto, Fast detection of penicillium rot and the conservation status of packaged citrus fruit using an optical array sensor, Chem. Commun. 60 (2024) 13702, https://doi.org/10.1039/D4CC04700A.

[24] R. Santonocito, A. Cavallaro, A. Pappalardo, R. Puglisi, A. Marano, M. Andolina, N. Tuccitto, G. Trusso Sfrazzetto, Detection of human salivary stress biomarkers using an easy-to-use array sensor based on fluorescent organic molecules, Biosens. Bioelectron. 270 (2025) 116986, https://doi.org/10.1016/j.bios.2024.116986.

[25] R. Santonocito, A. Cavallaro, R. Puglisi, A. Pappalardo, N. Tuccitto, M. Petroselli, G. Trusso Sfrazzetto, Smartphone-Based sensing of cortisol by functionalized rhodamine probes, Chem. Eur. J. 30 (2024) e202401201, https://doi.org/10.1002/chem.202401201.

[26] N. Tuccitto, S.O. Cacciola, F. Pappalardo, A. Cavallaro, NanoCom '24, 122–123 2024. https://doi.org/10.1145/3686015.3689362.

[27] R. Santonocito, M. Intravaia, I.M. Caruso, A. Pappalardo, G. Trusso Sfrazzetto, N. Tuccitto, Fluorescence sensing by carbon nanoparticles, Nanoscale Adv. 4 (2022) 1926–1948, https://doi.org/10.1039/D2NA00080F.

Alessia Cavallaro received the Master degree in Chemistry with 110/110 cum laude, working on multi-array sensors to detect stress biomarkers. She is currently a PhD student in Chemical Sciences, working on the development of new sensing devices for environmental security.

Rossella Santonocito received the Master degree in Chemical Sciences (curriculum Organic and Bioorganic Chemistry), in July 2021. Then, she received the PhD in Chemical Sciences, working on multi-array sensors to detect biomarkers of stress released in extreme environments. Actually, she is a Post-Doc at the University of Catania, working on new array devices for human health.

Andrea Pappalardo received the degree in Chemistry and Pharmaceutical Technologies at the University of Catania. From 2018 he is Associate Professor of Organic Chemistry. The research activity is focused on the synthesis of calixarene macrocycles and their use as catalysts in enantioselective epoxidations, and receptors in the supramolecolar host/guest chemistry.

Prof. Nunzio Tuccitto received his Ph.D. in chemistry in 2007. He is currently an associate professor of physical chemistry at the University of Catania, Italy. He studies the theoretical models governing molecular communication between implantable medical devices, synthesizes molecular messengers based on carbon nanoparticles, and develops bench-top prototypes to test communication. His research activity is also focused on developing nanoparticles for the detection of hazardous gases (e.g Warfare Agents and explosives), and monitoring of anthropogenic pollutants in the troposphere.

Giuseppe Trusso Sfrazzetto received the Master Degree in Chemistry (Organic and Bioorganic Chemistry, University of Catania) on 2007 and the PhD in Chemical Sciences on 2011. Actually, he is Associate Professor of Organic Chemistry in the Department of Chemical Sciences, in the University of Catania. His research activity is focused on the development of supramolecular sensors for human health and security.